Infiltration of circulating myeloid cells through CD95L contributes to neurodegeneration in mice

Liang Gao,[1]* David Brenner,[1]* Enric Llorens-Bobadilla,[1] Gonzalo Saiz-Castro,[1] Tobias Frank,[2] Peter Wieghofer,[3,4] Oliver Hill,[6] Meinolf Thiemann,[6] Saoussen Karray,[7] Marco Prinz,[3,5] Jochen H. Weishaupt,[8] and Ana Martin-Villalba[1]

[1]Division of Molecular Neurobiology, German Cancer Research Center (DKFZ), 69120 Heidelberg, Germany
[2]Department of Neurology, University Medical Center, Georg-August-University, 37075 Göttingen, Germany
[3]Institute of Neuropathology, [4]Faculty of Biology, and [5]BIOSS Centre for Biological Signalling Studies, University of Freiburg, 79098 Freiburg, Germany
[6]Apogenix GmbH, 69120 Heidelberg, Germany
[7]Institut National de la Santé et de la Recherche Médicale (INSERM), U1160, Université Paris Diderot, 75010 Paris, France
[8]Department of Neurology, University of Ulm, 89081 Ulm, Germany

Neuroinflammation is increasingly recognized as a hallmark of neurodegeneration. Activated central nervous system–resident microglia and infiltrating immune cells contribute to the degeneration of dopaminergic neurons (DNs). However, how the inflammatory process leads to neuron loss and whether blocking this response would be beneficial to disease progression remains largely unknown. CD95 is a mediator of inflammation that has also been proposed as an apoptosis inducer in DNs, but previous studies using ubiquitous deletion of CD95 or CD95L in mouse models of neurodegeneration have generated conflicting results. Here we examine the role of CD95 in 1-methyl-4-phenyl-1,2,3,6-tetrahydropyridin (MPTP)–induced neurodegeneration using tissue-specific deletion of CD95 or CD95L. We show that DN death is not mediated by CD95-induced apoptosis because deletion of CD95 in DNs does not influence MPTP-induced neurodegeneration. In contrast, deletion of CD95L in peripheral myeloid cells significantly protects against MPTP neurotoxicity and preserves striatal dopamine levels. Systemic pharmacological inhibition of CD95L dampens the peripheral innate response, reduces the accumulation of infiltrating myeloid cells, and efficiently prevents MPTP-induced DN death. Altogether, this study emphasizes the role of the peripheral innate immune response in neurodegeneration and identifies CD95 as potential pharmacological target for neurodegenerative disease.

CORRESPONDENCE
Ana Martin-Villalba:
a.martin-villalba@dkfz.de

Abbreviations used: BBB, blood–brain barrier; CNS, central nervous system; DA, dopamine; DN, dopaminergic neuron; DOPAC, 3,4-dihydroxyphenylacetic acid; EAE, experimental autoimmune encephalitis; HVA, homovanillic acid; MPP, 1-methyl-4-phenylpyridinium; MPTP, 1-methyl-4-phenyl-1,2,3,6-tetrahydropyridin; PD, Parkinson's disease; SNpc, substantia nigra pars compacta; TH, tyrosine hydroxylase; VTA, ventral tegmental area.

Idiopathic Parkinson's disease (PD) is the second most frequent neurodegenerative disorder. Current medical treatments are only able to provide partial symptomatic relief of the major motor symptoms, namely rigor, tremor, and akinesia. Only in a minority of all PD patients is a familial mutation known to be the cause of the disease, whereas ∼90% of all PD cases are idiopathic. Mitochondrial dysfunction, oxidative stress, and impaired degradation of proteins have been proposed as possible etiology of idiopathic PD (Dauer and Przedborski, 2003). Accordingly, environmental exposure to neurotoxic pesticides increases the risk of developing PD, and indeed, intoxication with the dopaminergic toxin 1-methyl-4-phenyl-1,2,3,6-tetrahydropyridin (MPTP) elicits PD in humans, primates, and rodents and represents a well-characterized toxin-based mouse model for PD (Dauer and Przedborski, 2003). In addition, increasing evidence from genome-wide association (Ahmed et al., 2012), epidemiological (Gao et al., 2011), postmortem, and animal model studies indicate that neuroinflammation, including glial activation, release of proinflammatory factors, and T cell

*L. Gao and D. Brenner contributed equally to this paper.

The Rockefeller University Press $30.00
J. Exp. Med. 2015 Vol. 212 No. 4 469–480
www.jem.org/cgi/doi/10.1084/jem.20132423

infiltration (Brochard et al., 2009) are actively involved in PD progression. Activation of microglia is also observed after MPTP intoxication, thus enabling investigators to study neurodegeneration-related inflammation (Członkowska et al., 1996; Hayley et al., 2004).

At the histopathology level, PD is characterized by a slow and progressive degeneration of dopaminergic neurons (DNs) in the substantia nigra pars compacta (SNpc), which exhibit accumulation of misfolded proteins. Apoptotic death of DNs has been observed both in postmortem samples of PD patients and in MPTP-intoxicated mice (Venderova and Park, 2012). The CD95/CD95 ligand (CD95L) system was discovered as a paradigmatic trigger of apoptosis, and thus, expression of these proteins has been characterized in preclinical models of PD and PD patients. Levels of CD95 protein and mRNA are higher in PD patients than in healthy individuals (Mogi et al., 1996; Simunovic et al., 2009). Therefore, this system was hypothesized to induce apoptosis of DNs. To address this issue, MPTP-mediated DN neurodegeneration was studied in mice with a targeted ubiquitous deletion of CD95 (*Fas null*) and in mice with a global spontaneous mutation in CD95 (*lpr*) or CD95L (*gld*). Although CD95-deficient mice (*FAS null*) exhibit attenuated loss of dopaminergic SNpc neurons as well as attenuated microglial activation in the SNpc in response to MPTP (Hayley et al., 2004), MPTP neurotoxicity is exacerbated in *lpr* and *gld* mice (Landau et al., 2005). These opposite outcomes underline the problem of using animal models with a global deletion of CD95 or CD95L for the study of tissue-specific pathologies. A global deficiency of either CD95 or CD95L causes a lymphoproliferative disorder that is present to a variable degree and in an age-dependent manner in each mutant mouse line, which hampers interpretation and comparison of experimental results (Roths et al., 1984; Adachi et al., 1996; Karray et al., 2004; Martin-Villalba et al., 2013).

Available tissue-specific mutant mice have greatly advanced our understanding of the role of the CD95/CD95L system in disease. This is best exemplified by studies on the role of CD95 in spinal cord injury. First experiments using mouse mutants ubiquitously deficient in CD95 or CD95L showed that these mice were protected against spinal cord injury, suggesting that triggering of CD95 in neurons induces apoptosis (Demjen et al., 2004). Later experiments showed that neuroprotection was caused by abrogation of neuroinflammation and not by inhibition of direct CD95-mediated neuronal apoptosis (Letellier et al., 2010). CD95 activity is used by macrophages and neutrophils to migrate to the injury site, and inhibition of CD95-mediated inflammatory infiltration decreases neuronal death. This and other studies highlight that the CD95 receptor fulfils diverse functions in different tissues in vivo beyond apoptosis (Martin-Villalba et al., 2013). In the central nervous system (CNS), it is involved in axonal outgrowth and adult neurogenesis, as well as migration of malignant glioblastoma cells (Desbarats et al., 2003; Zuliani et al., 2006; Kleber et al., 2008; Corsini et al., 2009). While in the immune system, it mediates survival, proliferation, and activation of T cells (Peter et al., 2007) and myeloid cell recruitment to inflammatory sites (Letellier et al., 2010).

To tease out the actual role of CD95 in PD, we used mutant mice deficient in CD95 in DNs or in peripheral myeloid cells and systemic pharmacological inhibition of CD95's activity. Here, we report that lack of CD95 in DNs does not render mice resistant to MPTP-induced toxicity. In contrast, exclusive deletion of CD95L in peripheral myeloid cells significantly attenuates loss of DNs in mice intoxicated with MPTP. Neuroprotection was also achieved by pharmacological inhibition of CD95L, which hampered infiltration of the brain by peripheral myeloid cells. Thus, this study underscores the contribution of peripheral inflammation to neurodegeneration in a mouse model of PD and identifies inhibition of CD95 as potential systemic therapy for PD patients.

RESULTS AND DISCUSSION

Neuronal CD95 activity is not involved in MPTP-induced neurodegeneration

To elucidate whether lack of CD95 in DNs exacerbates or attenuates MPTP-induced DN death in vivo, we generated mice with specific deletion of CD95 in DNs (hereafter referred to as $CD95^{f/f;DATcre}$ mice; Fig. 1 A). To this end, saline or a subacute dose of 30 mg/kg MPTP per day was administered for five consecutive days to $CD95^{f/f;DATcre}$ mice or their control littermates. 6 d after the last injection of MPTP, the number of tyrosine hydroxylase (TH)–positive (TH^+) DNs in SNpc and the striatal dopamine (DA) metabolite levels were quantified (Fig. 1, B–E). First, the number of TH^+ DNs in SNpc and ventral tegmental area (VTA) was not influenced by the deletion of CD95, as it was similar in nontreated $CD95^{f/f;DATcre}$ and control counterparts. Importantly, MPTP-exposed $CD95^{f/f}$ and $CD95^{f/f;DATcre}$ groups exhibited significantly reduced numbers of TH^+ neurons in SNpc when compared with saline-treated controls. Thus, CD95 deficiency in DNs does not influence MPTP-induced toxicity of nigral DNs (Fig. 1 C). Count of $Nissl^+$ cells confirmed that reduction of TH^+ cell number was not caused by down-regulation of TH expression (not depicted). To further evaluate whether the lack of neuroprotection through loss of CD95 in DNs is caused by changes in DA metabolism, striatal levels of DA and its metabolites 3,4-dihydroxyphenylacetic acid (DOPAC) and homovanillic acid (HVA) were determined using HPLC. As shown in Fig. 1 (D and E), striatal DA levels as well as the metabolite ratio [(DOPAC + HVA)/DA] did not differ between $CD95^{f/f;DATcre}$ and control counterparts after application of MPTP. Altogether, these data allow the conclusion that death of DNs is not directly mediated by CD95 activity in DNs. This observation is in line with our previous findings showing that neurodegeneration in an animal model of spinal cord injury is not prevented by the lack of CD95 in neurons (Letellier et al., 2010).

Brochard et al. (2009) recently reported that $CD4^+$ T cell–deficient mice exhibit reduced degeneration of SNpc DNs after MPTP intoxication. Interestingly, microglial activation is almost completely abolished in these mice. In addition,

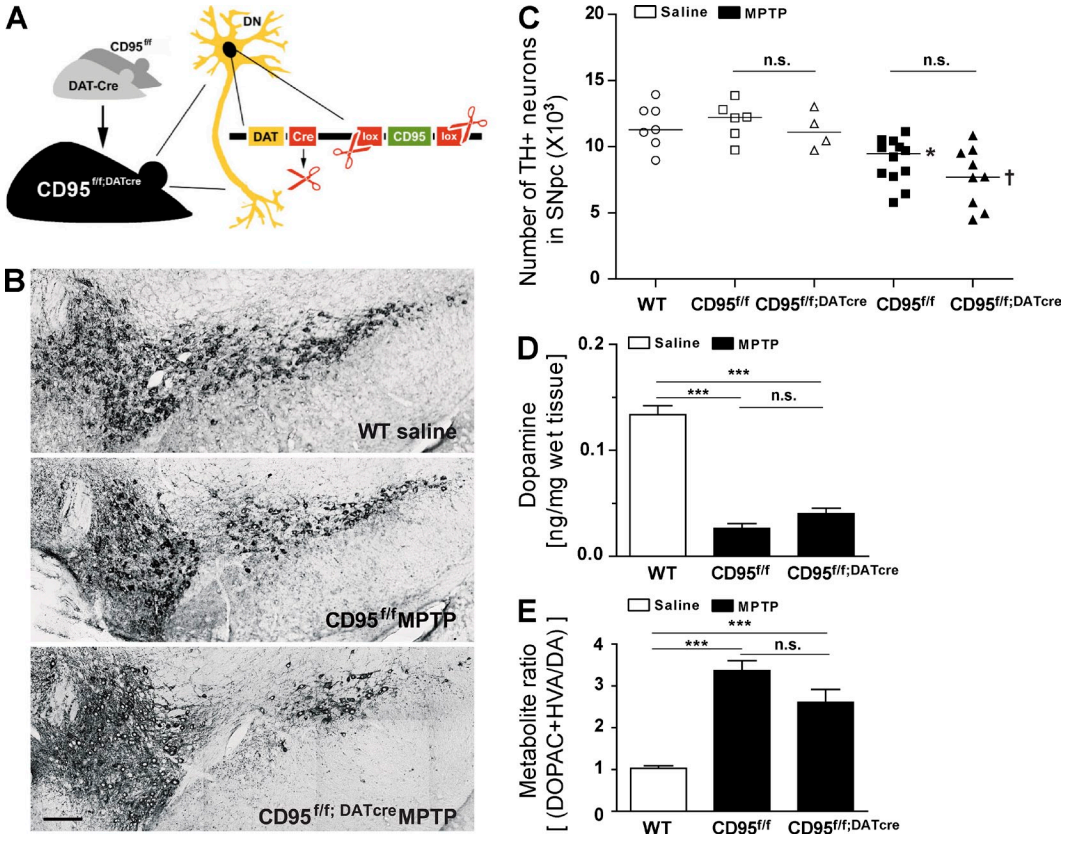

Figure 1. Selective deletion of CD95 in DNs (*CD95*$^{f/f;DATcre}$ mice) does not influence dopaminergic neurodegeneration after treatment with MPTP. (A) Scheme of *CD95*$^{f/f;DATcre}$ mice. (B) Representative images of TH$^+$ neurons in SNpc of control and *CD95*$^{f/f;DATcre}$ mice. Bar, 100 µm. (C) Quantification of total TH$^+$ DNs in the SNpc at day 6 after last administration of saline or MPTP to WT, *CD95*$^{f/f}$, or *CD95*$^{f/f;DATcre}$ mice. Data are presented as dot plot with median; $n = 4–12$. ANOVA followed by Newman–Keuls post-hoc test: *CD95*$^{f/f}$ versus *CD95*$^{f/f}$ + MPTP: **, $P < 0.01$; *CD95*$^{f/f;DATcre}$ versus *CD95*$^{f/f;DATcre}$ + MPTP: †, $P < 0.01$; n.s., not significant. (D and E) Quantification of DA metabolite levels and metabolite ratio in striatum at day 6 after last administration of MPTP in saline-treated WT, MPTP-treated *CD95*$^{f/f}$, and *CD95*$^{f/f;DATcre}$ mice. Data are presented as mean ± SEM; $n = 6–7$. ANOVA followed by Newman–Keuls post-hoc test: ***, $P < 0.001$.

T cell–deficient mice reconstituted with splenic T cells from CD95L-deficient *gld* donor mice were equally protected, thus suggesting that CD95L is required for CD4$^+$ T cell–mediated dopaminergic toxicity. The authors suggested that CD4$^+$ T cells could participate in the inflammatory reaction by activating innate immune cells or astrocytes via CD95L. Indeed, increased expression of CD95 is reported in these glial cells both in PD patients and in the MPTP model (Ferrer et al., 2000; Hayley et al., 2004).

Deletion of CD95L in the myeloid cell lineage attenuates MPTP-induced neurodegeneration

To address the contribution of CD95L expressed on myeloid cells in general to MPTP-induced neurodegeneration, we took advantage of mice deficient in CD95L in the myeloid lineage (monocytes/macrophages, microglia, and neutrophils; mice hereafter referred to as *CD95L*$^{f/f;LysMcre}$; Fig. 2 A). CD95L deletion was confirmed by genome DNA quantitative PCR of FACS-sorted neutrophils and monocyte samples (not depicted). 6 d after the last MPTP injection, remaining TH$^+$ DNs and accumulation of CD11b$^+$ cells in SNpc were assessed by immunohistochemistry. *CD95L*$^{f/f}$ control mice exhibited a 25% loss of SNpc TH$^+$ neurons as compared with saline-treated *CD95L*$^{f/+;LysMcre}$ mice. In contrast, *CD95L*$^{f/f;LysMcre}$ mice were protected against MPTP-induced neurodegeneration (Fig. 2, B and C).

Microgliosis has been associated with neurodegeneration, and several studies have reported robust microgliosis in the SNpc of MPTP-intoxicated mice (reviewed by McGeer and McGeer [2008]). Hence, we assessed whether accumulation of CD11b$^+$ microglia cells in SNpc was altered in *CD95L*$^{f/f;LysMcre}$ mice. Microglia belong to the myeloid lineage (Ransohoff and Cardona, 2010), and Cre-mediated recombination occurs in activated microglia in *LysM-cre*$^+$ mice (Cho et al., 2008; Ros-Bernal et al., 2011; Goldmann et al., 2013), suggesting that microglia in neuroprotected *CD95L*$^{f/f;LysMcre}$ mice are CD95L deficient. In line with a previous study, MPTP-treated littermate controls showed manifest accumulation of activated microglia with a round and thickened shape (Hayley et al., 2004). However, MPTP-treated *CD95L*$^{f/f;LysMcre}$ mice exhibited minimal CD11b immunoreactivity, with microglia

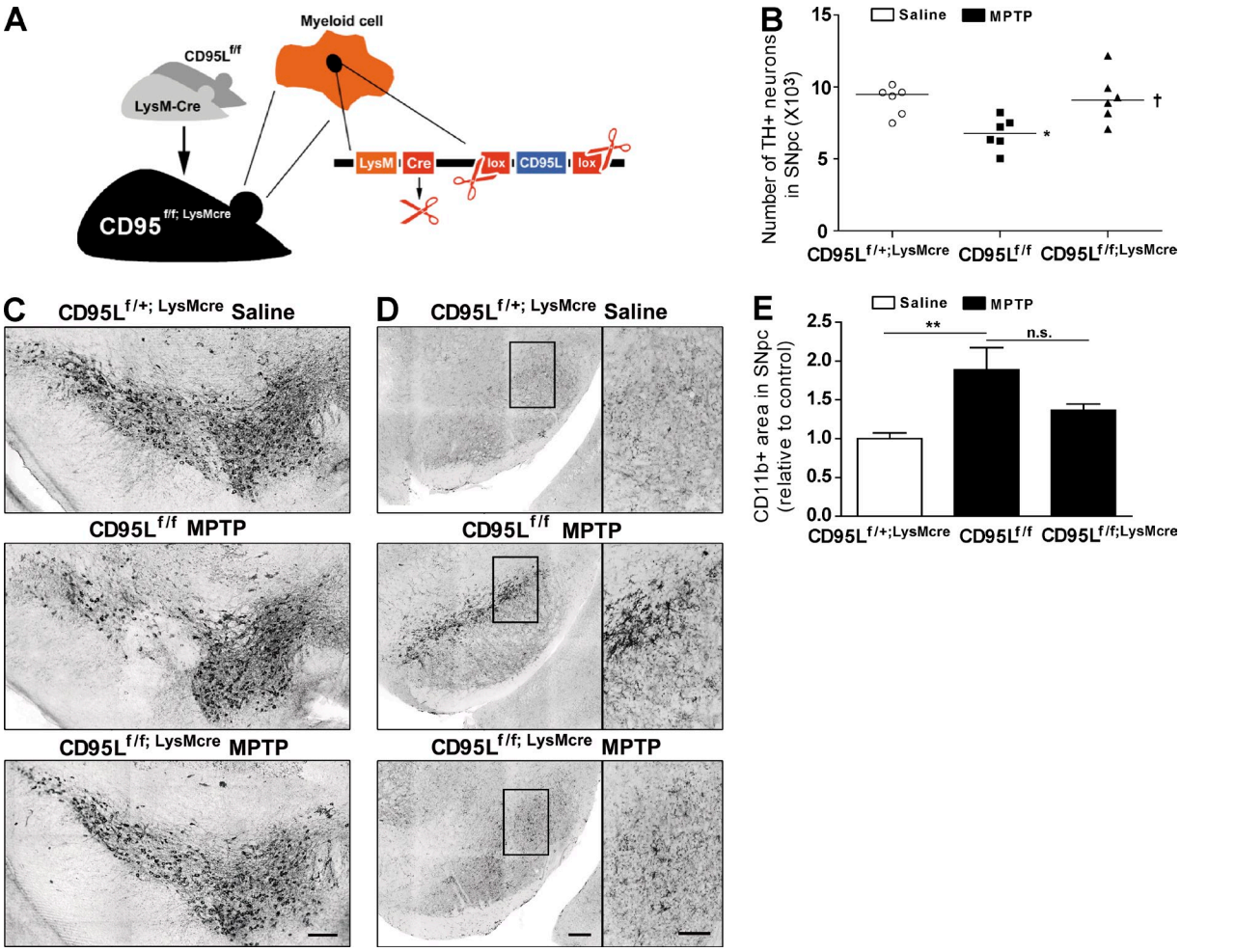

Figure 2. Mice with deletion of CD95L in myeloid cells (*CD95L*$^{f/f;LysMcre}$ mice) are more resistant to MPTP. (A) Scheme of *CD95L*$^{f/f;LysMcre}$ mice. (B) Quantification of total TH$^+$ DNs in the SNpc at day 6 after last administration of saline or MPTP to *CD95L*$^{f/+;LysMcre}$, *CD95*$^{f/f}$, or *CD95L*$^{f/f;LysMcre}$ mice. Data are presented as dot plot with median; $n = 6$. ANOVA followed by Newman–Keuls post-hoc test: control versus *CD95L*$^{f/f}$: *, $P < 0.01$; *CD95L*$^{f/f}$ versus *CD95L*$^{f/f;LysMcre}$: †, $P < 0.05$. (C) Representative images of TH$^+$ neurons in SNpc of control and *CD95L*$^{f/f;LysMcre}$ mice. (D) Representative photomicrographs of SNpc sections immunostained with anti-CD11b from control and *CD95L*$^{f/f;LysMcre}$ mice. Note the different morphology of CD11b$^+$ cells in *CD95L*$^{f/f}$ and *CD95L*$^{f/f;LysMcre}$ mice, as shown in the magnified pictures of anti-CD11b staining in the insets in SNpc. Bars: (C and D) 100 µm (D, insets) 50 µm. (E) Quantification of CD11b$^+$ cells in SNpc. Data are presented as mean ± SEM; $n = 6$. ANOVA followed by Newman–Keuls post-hoc test: **, $P < 0.01$; n.s., not significant.

showing a ramified shape characterized by thin processes, which are indicative of an inactive state (Fig. 2, D and E).

Thus, these findings provide a causal link between myeloid cells, and particularly the CD95L from myeloid cells, and dopaminergic neurodegeneration. Consistent with these results, mice with ubiquitous CD95 deficiency (*Fas null*) show reduced dopaminergic neurodegeneration and attenuated microglial activation in response to subacute MPTP (Hayley et al., 2004). Microglial activation and release of proinflammatory factors have been clearly associated with degeneration of SNpc DNs (Liberatore et al., 1999; Wu et al., 2002). Activation of microglia in turn leads to up-regulation of CD95L in vivo (Terrazzino et al., 2002) and increased release of soluble CD95L in vitro (Taylor et al., 2005). Therefore, it cannot be excluded that CD95L may also activate microglia and thereby contribute through other effector molecules to kill DNs.

Pharmacological neutralization of CD95L protects mice against MPTP toxicity and alters peripheral immune response

CD95L$^{f/f;LysMcre}$ mice lack CD95L in the whole myeloid lineage, including peripheral myeloid cells. Therefore, CD95L in circulating myeloid cells could be involved in the pathogenesis of PD. Notably, in the experimental autoimmune encephalitis (EAE) mouse model, the myeloid compartment does not only embrace resident microglia, but also peripheral monocytes (Ajami et al., 2011). The pathogenic significance of circulating myeloid cells, and in particular of inflammatory monocytes, which in turn infiltrate the lesion site, is increasingly appreciated in inflammation-associated diseases (Mildner et al., 2009). In mice,

inflammatory Ly6C$^+$CCR2$^+$CX3CR1^{lo} (Ly6C^{hi}) monocytes can be distinguished from Ly6C$^-$CCR2$^-$CX3CR1^{hi} (Ly6C^{lo}) resident monocytes that are thought to correspond to human classical (CD14$^+$CD16$^-$CD64$^+$) monocytes (Cros et al., 2010; Yona and Jung, 2010). Inhibition of monocyte accumulation at inflammatory sites by lineage depletion or siRNA silencing of CCR2 mRNA in monocytes alleviates symptoms in several inflammation-associated cardiovascular disease mouse models (Leuschner et al., 2011). And also in PD patients, strong up-regulation in the percentage of peripheral blood monocyte precursors (CFU-Ms) and surface CCR2 levels was observed in classical monocytes (Funk et al., 2013). In the MPTP model, studies using lethal irradiation and BM reconstitution with GFP$^+$ donor cells have suggested that BM-derived cells infiltrate the CNS and differentiate to microglia-like cells, thus contributing to neuroinflammation (Kokovay and Cunningham, 2005; Rodriguez et al., 2007). However, the validity of these reconstitution studies has been questioned. Mildner et al. (2007) recently demonstrated that irradiation in conjunction with the process of BM reconstitution activates the competence of reconstituted cells to cross the blood–brain barrier (BBB) and engraft in the CNS of healthy hosts. By applying a combination of parabiosis and myeloablation, another study revealed that, contrary to studies using BM transplantation, in healthy and even in EAE diseased mice CNS microglia are not replenished by BM-derived progenitors but can self-renew lifelong (Ajami et al., 2011). Using this approach to investigate pathogenic involvement of myeloid cells in various CNS diseases, they demonstrated that circulating monocytes infiltrate the CNS of mice with EAE and that infiltration strongly correlated with EAE progression to the paralytic stage. However, in the long term, monocytes do not contribute to the resident microglia pool in EAE. Interestingly, Ly6C^{hi} monocytes already accumulate in the blood and CNS during the preclinical stage in EAE mice (Mildner et al., 2009). In addition, the pathogenic significance of circulating monocytes has most recently been shown in the SOD1 mouse model for ALS by Butovsky et al. (2012). Using flow cytometric analysis, they revealed that circulating inflammatory monocytes are recruited to the spinal cord and monocyte infiltration correlates with neuronal loss. Treatment with anti-Ly6C mAb reduces monocyte infiltration, neuronal loss, and increases survival time in SOD1 mice (Butovsky et al., 2012). Notably, Ly6C^{hi} monocytes in the spleen show a proinflammatory profile in the early presymptomatic stage of disease. Previously, we have shown that neutralization of CD95L inhibits recruitment of peripheral myeloid cells to the injured spinal cord, thereby alleviating neuronal loss (Letellier et al., 2010). Thus, the neuroprotective effect we observed by CD95L deficiency in MPTP-intoxicated *CD95L$^{f/f;LysMcre}$* mice might also arise from reduced recruitment of circulating myeloid cells in SNpc.

To test this hypothesis, we treated WT mice with a stable CD95-Fc fusion protein that neutralizes CD95 activity and does not cross the BBB (CD95-Fc hereafter referred to as APG112; Fig. 3 A). Accordingly, APG112 was not detected in the brain tissue of MPTP-treated mice but only endovascular in the brain of MPTP + APG–treated mice (not depicted). Thus, the CD95-Fc main site of action is in the periphery, and therefore, it can be used to distinguish between the contribution of neurodegeneration of peripheral myeloid cells and resident microglia. 6 d after the last MPTP injection, we analyzed brains and blood of saline- and MPTP-treated mice. Mice that received saline showed a significant reduction of DNs upon MPTP intoxication, whereas, similar to *CD95L$^{f/f;LysMcre}$* mice, mice that had been systemically treated with APG112 were resistant to MPTP-induced degeneration of SNpc DNs. Altogether, these data demonstrate that CD95L neutralization is neuroprotective in a mouse model of DN degeneration (Fig. 3, B and C).

Furthermore, after MPTP intoxication, mice that were injected with APG112 exhibited slightly higher striatal DA levels than saline-treated counterparts (Fig. 3 D). In addition, the metabolite ratio [(DOPAC + HVA/DA) × 100] was significantly lower in the APG112 treatment group than in the saline-treated one, implying that treatment with APG112 protected DNs (Fig. 3 E). MPTP toxicity depends on the enzymatic conversion of MPTP to 1-methyl-4-phenylpyridinium (MPP) ion (MPP$^+$) by monoamine oxidase. To exclude the possibility that administration of APG112 affects MPTP metabolism, we measured striatal MPP$^+$ levels 90 min after MPTP application. Similar levels of MPP$^+$ levels were observed in saline-treated control mice and APG112-treated mice, indicating that MPTP metabolism is not influenced by APG112 treatment (Fig. 3 F).

To elucidate the effect of CD95L neutralization on monocyte recruitment in PD mice, we measured the blood monocyte levels by flow cytometry (Fig. 3 G). The number of Ly6C^{hi} inflammatory monocytes was significantly higher in MPTP-intoxicated WT mice than in saline-treated controls (Fig. 3 H). Remarkably, in MPTP-intoxicated mice that received APG112 (WT + APG112 mice), the fraction of Ly6C^{hi} monocytes remained at saline control levels. The proportion of the Ly6C^{lo} monocyte subset was not affected in either the saline-treated or the MPTP-intoxicated group.

Mice with deletion of CD95L in peripheral myeloid cells are resistant to MPTP neurotoxicity

To confirm that infiltrating peripheral myeloid cells are the major source of CD95L contributing to striatal degeneration, we set out to perform MPTP experiments with BM chimeras. However, chimeric mice generated from BM transplantation after whole body irradiation demonstrate disadvantages for studying the involvement of BM-derived cells in CNS diseases, such as induction of proinflammatory cytokines in the brain (Mildner et al., 2007; Kierdorf et al., 2013b) and disruption of the BBB, which leads to the engraftment of BM-derived cells in healthy conditions (Priller et al., 2001; Diserbo et al., 2002). Interestingly, an approach using head-shielded (protected CNS) irradiation has been shown to overcome these problems (Mildner et al., 2007, 2011). Therefore, we generated *CD95L$^{f/f;LysMcre}$* BM chimeras in which the heads

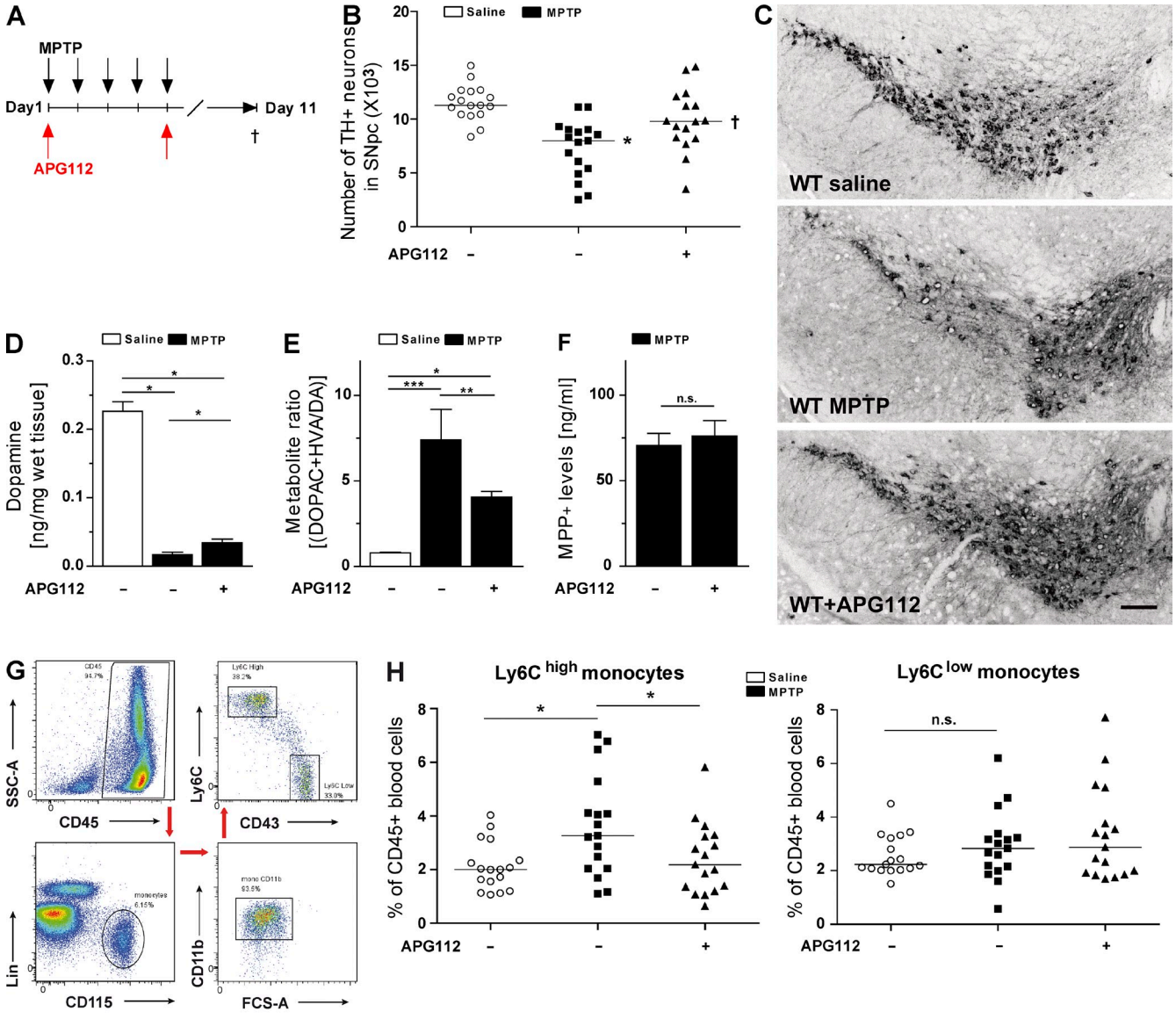

Figure 3. Pharmacological neutralization of CD95L protects mice against MPTP toxicity and alters peripheral immune response. (A) Scheme of MPTP and APG112 treatment. (B) Quantification of total TH⁺ DNs in the SNpc at day 6 after last administration of saline or MPTP of control or APG112-treated mice. ANOVA followed by Newman–Keuls post-hoc test: control versus MPTP: *, $P < 0.001$; MPTP versus MPTP + APG112: †, $P < 0.01$. (C) Representative images of TH⁺ neurons in SNpc of control and APG112-treated mice. Bar, 100 µm. (D) Quantification of striatal DA levels using HPLC at day 6 after last administration of saline or MPTP to control or APG112-treated mice. (E) Calculation of the metabolite ratio [(DOPAC + HVA/DA) × 100] after quantification of striatal DA metabolite levels by HPLC. (D and E) Data are presented as mean ± SEM; $n = 8$. ANOVA on ranks, Student–Newman–Keuls multiple comparison: *, $P < 0.05$; **, $P < 0.01$; ***, $P < 0.001$. (F) HPLC measurement of striatal MPP⁺ levels in WT and WT + APG112 mice at 90 min after MPTP injection. Data are presented as mean ± SEM; $n = 3$. Student's t test: n.s., not significant. (G) Representative dot plots of blood monocytes and gating scheme of flow cytometry. (H) Quantification of blood monocyte subsets by FACS at day 6 after last administration of saline or MPTP of control or APG112-treated mice. ANOVA followed by Newman–Keuls post-hoc test: *, $P < 0.05$. (B and H) Data are presented as dot plot with median and were pooled from two independent experiments; $n = 16–17$.

of the recipient animals were protected from the irradiation before BM transplantation (Fig. 4 A). In these mice, the microglia were WT (CD45.1) and circulating blood cells were majorly derived from the *CD95L*$^{f/f;LysMcre\pm}$ (CD45.2) donor BM. As the BM in the skull was protected from irradiation, donor BM–derived blood cells (CD45.2⁺) constituted 75% of all CD45⁺ blood cells in the chimeras 8 wk after reconstitution, which was comparable with our previous data (Fig. 4, B and C; Mildner et al., 2007). Upon MPTP treatment, peripheral CD95L deletion in *CD95L*$^{f/f;LysMcre}$ chimeras significantly rescued DNs from neurotoxicity as compared with control *CD95L*$^{f/f}$ chimeras (Fig. 4 D). These experiments suggest that CD95L in peripheral myeloid cells is an essential mediator of dopaminergic degeneration.

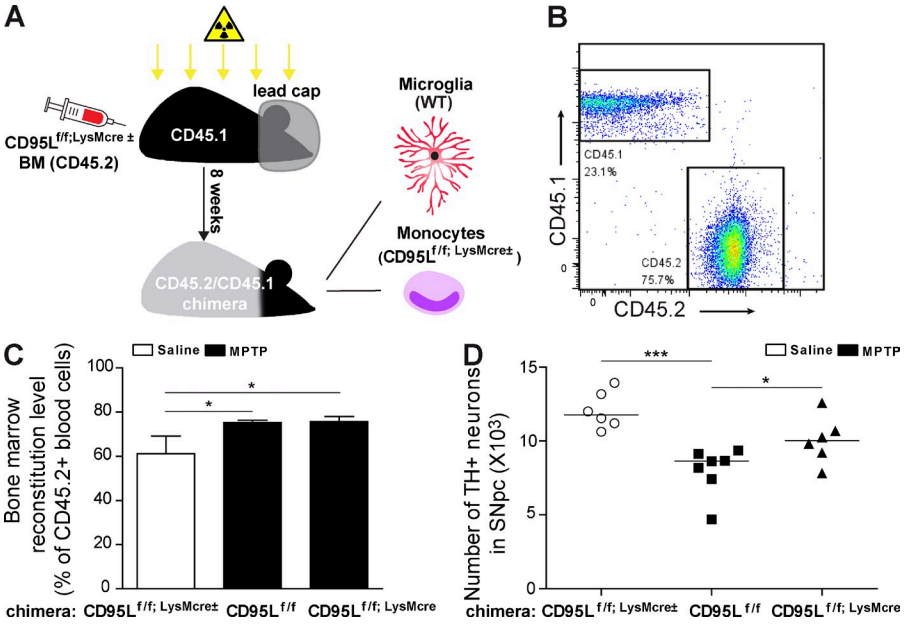

Figure 4. Mice with deletion of CD95L in peripheral myeloid cells (*CD95L*$^{f/f;LysMcre}$ chimera mice) are resistant to MPTP neurotoxicity. (A) Scheme of *CD95L*$^{f/f;LysMcre}$ BM chimera mice. The heads of BM recipient mice were covered with a lead cap during irradiation to avoid irradiation-induced monocyte infiltration. (B) Representative FACS dot plots of CD45.1- and CD45.2-stained blood samples from *CD95L*$^{f/f;LysMcre±}$ BM chimera mice. (C) BM reconstitution level of chimera mice before the injection of saline or MPTP. Data are presented as mean ± SEM; $n = 6–7$. (D) Quantification of total TH+ DNs in the SNpc at day 6 after last administration of saline or MPTP to *CD95L*$^{f/f;LysMcre±}$ BM chimera mice. Data are presented as dot plot with median; $n = 6–7$. (C and D) ANOVA followed by Newman–Keuls post-hoc test: *, $P < 0.05$; ***, $P < 0.001$.

Neutralization of CD95L reduces infiltration of circulating myeloid cells in SNpc

The origin of microglia has been a matter of debate for several decades. Recent studies show conclusively that adult microglia derive from yolk sac myeloid progenitors at E8 and are distinct from monocyte-derived macrophages (Ginhoux et al., 2010; Schulz et al., 2012; Kierdorf et al., 2013a). Despite the difference in developmental origin, microglia share similar features with other myeloid cells such as the expression of Fc, complement receptors, CD11b, F4/80, CX3CR1, and other epitopes typically expressed by myeloid monocytes (Prinz and Mildner 2011). These features make it difficult to distinguish infiltrating monocytes from microglia simply by immunostaining.

Although microglia share very similar surface markers as circulating monocytes, accumulating evidence shows that some molecules can be used to distinguish them from each other. Expression of $P2Y_{12}$, a metabotropic purinergic receptor, was observed in central microglia but not in peripheral myeloid cells (Haynes et al., 2006). Interestingly, a recent study based on gene profiling and quantitative mass spectrometry analysis of $CD11b^+CD45^{lo}$ microglia isolated from the CNS and $CD11b^+Ly6C^+$ monocytes isolated from the spleen demonstrated that $P2Y_{12}$ is uniquely and highly expressed in microglia but not in circulating monocytes (Butovsky et al., 2014). These studies indicate that $P2Y_{12}$ can be used as a marker to distinguish myeloid cell–derived microglia from CNS-resident microglia.

To analyze circulating monocyte infiltration in DN degeneration, we analyzed infiltration of circulating innate immune cells into SNpc in MPTP-intoxicated mice by assessment of CD11b/P2Y12 expression. As shown in Fig. 5 (A and B), CNS-resident microglia are $P2Y_{12}$ and CD11b double positive and engrafted myeloid cells are CD11b single positive. CD11b single-positive cells were not detected in SNpc or VTA of saline-treated mice. However, in MPTP-intoxicated mice, infiltrating CD11b single-positive cells accumulated in the SNpc and VTA. These data suggest that these cells are peripheral myeloid cells. Most importantly, we found that APG112 treatment significantly reduced the MPTP-mediated infiltration of circulating myeloid cells in the SNpc and VTA (Fig. 5 C).

Moreover, the monocyte marker CD169 (*Siglec1*) has been shown to be expressed only by recruited BM-derived monocytes, but not by microglia in a mouse model of amyotrophic lateral sclerosis (Butovsky et al., 2012). In MPTP-treated mice, we observed CD169-positive cells in SNpc, which further proved monocyte infiltration during DNs degeneration (Fig. 5, D–H).

To further confirm the peripheral myeloid cell infiltration, we used the recently established *Cx3cr1*^{creER}:*Rosa26(R26)-yfp* reporter mice, a new animal tool to study the distinct functions of microglia compared with infiltrating monocytes (Goldmann et al., 2013). Upon the pulse induction using tamoxifen, microglia and circulating monocytes are efficiently labeled with YFP. However, as monocytes have a shorter lifetime and microglia persist through lifetime, circulating YFP^+ monocytes are replaced by nonlabeled cells 4 wk after tamoxifen induction, and microglia still express the YFP reporter. Taking this advantage, we crossed *Cx3cr1*^{creER} mice with *Rosa26(R26)*-tdTomato mice (hereafter referred to as tdTomato$^{R26f/f;Cx3cr1creER}$ mice) and treated them 6 wk after tamoxifen induction with MPTP and APG112 to investigate the role of CD95L on monocyte infiltration in DN degeneration (Fig. 6 A). The infiltrating monocytes were unambiguously identified as $CD11b^+tdTomato^-$ cells in contrast to $CD11b^+tdTomato^+$ microglia. In MPTP-treated mice,

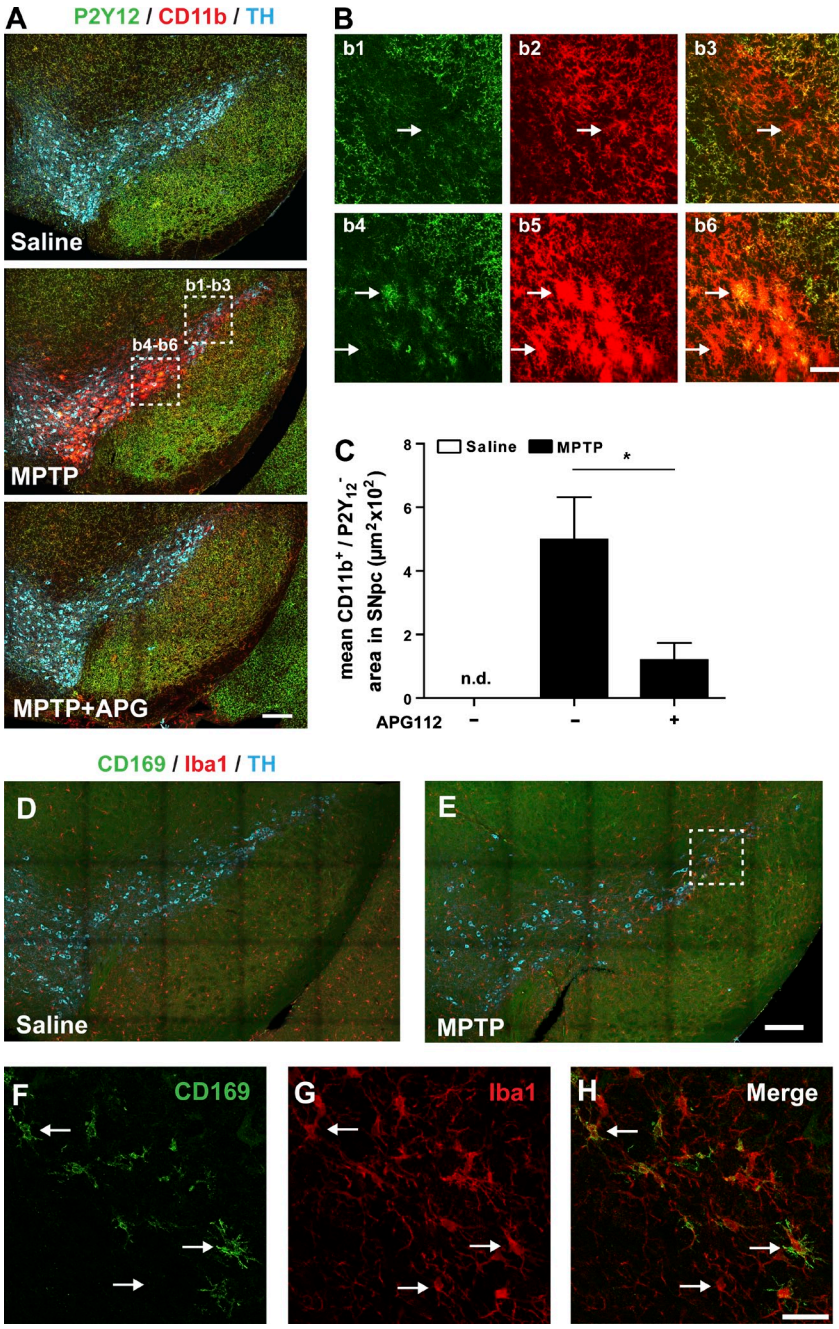

Figure 5. Myeloid cell infiltration in SNpc demonstrated by staining of microglia marker $P2Y_{12}$ or monocyte marker CD169. (A) Representative photomicrographs of SNpc sections immunostained with anti-$P2Y_{12}$, anti-TH, and anti-CD11b from saline-, MPTP-, and MPTP + APG112–treated mice. (B) Representative CD11b single-positive ($CD11b^+/P2Y_{12}^-$; as indicated with arrows in b1–b3) and CD11b $P2Y_{12}$ double-positive ($CD11b^+/P2Y_{12}^+$; as indicated with arrows in b4–b6) cells, which are highlighted with dashed rectangles in A. (C) Mosaic acquisition of CD11b single-positive ($CD11b^+/P2Y_{12}^-$) area in saline-, MPTP-, and MPTP/APG112-treated mice. Data are presented as mean ± SEM; $n = 10$. Student's t test: *, $P < 0.05$; n.d., not detectable. (D and E) Representative photomicrographs of SNpc sections immunostained with anti-CD169, anti-Iba1, and anti-TH from saline- and MPTP-treated mice. Infiltrating monocytes are $CD169^+/Iba1^+$ cells and microglia are $CD169^-/Iba1^+$ cells, as arrows indicate in F–H (dashed rectangle in E). Bars: (A, D, and E) 100 µm; (B) 30 µm; (F–H) 20 µm.

$CD11b^+tdTomato^-$ infiltrating monocytes were observed in SNpc (Fig. 6 B). More importantly, the monocyte infiltration was significantly blocked by APG112 treatment (Fig. 6 C).

Collectively, our findings provide evidence that circulating myeloid cells are involved in aggravation of neurodegeneration in MPTP-intoxicated mice. Importantly, systemic neutralization of CD95L prevented destruction of SNpc DNs. It remains to be elucidated whether this effect was predominantly based on inhibition of peripheral innate or adaptive cellular immunity. Although CD95L deletion in myeloid cells or APG112 blockade has no obvious impact on $CD4^+$ T cells level in blood of MPTP-intoxicated mice (unpublished data), future studies will have to address whether the CD95-driven myeloid cell infiltration in brain is regulated by T cells.

It is also of great significance to investigate whether infiltrating myeloid cells are involved in disease progression of PD patients. Interestingly, a recent publication reported that classical monocytes were enriched in the blood of PD patients and demonstrated a pathological hyperactivity, which correlated with disease severity (Grozdanov et al., 2014). Using a next-generation sequencing approach, it was found that PD monocytes exhibited a dysregulation of inflammatory pathways, and CD95 was identified as one of the critical mediators

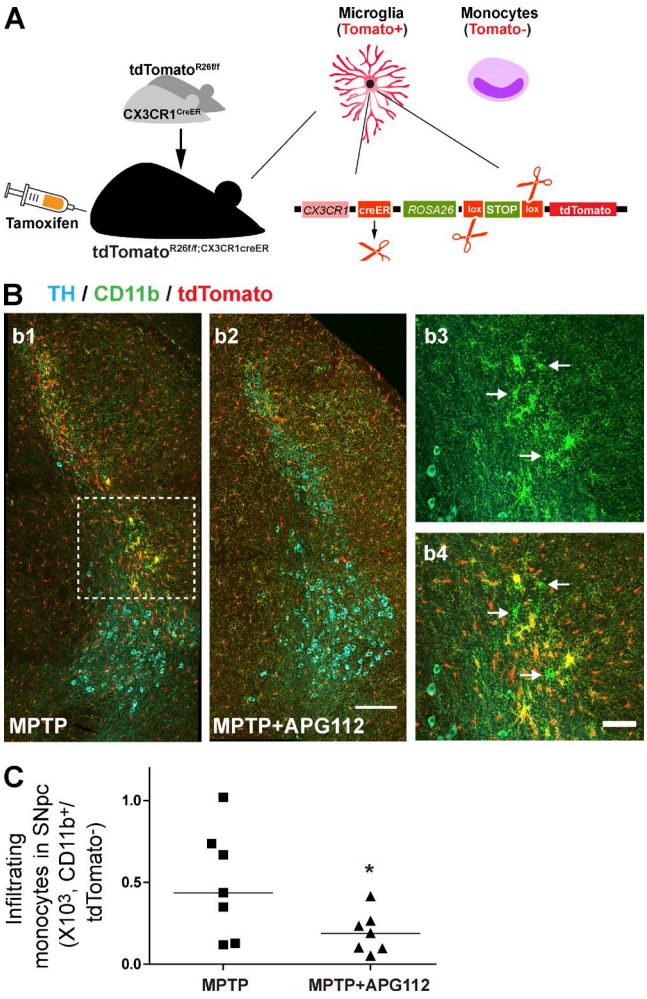

Figure 6. Pharmacological neutralization of CD95L reduces infiltration of circulating myeloid cells in SNpc. (A) Scheme of tdTomato$^{R26f/f;Cx3cr1creER}$ mice. 4 wk after tamoxifen induction, microglia were tdTomato positive and the circulating monocytes were tdTomato negative. (B) Representative CD11b single-positive (CD11b^{+}/tdTomato^{-}; as indicated with arrows in b3 and b4) infiltrating monocytes, which are highlighted with the dashed rectangle in b1. Bars: (b1 and b2) 50 µm; (b3 and b4) 20 µm. (C) Quantification of infiltrating monocytes (CD11b^{+}/tdTomato^{-}) in SNpc of MPTP- and MPTP/APG112-treated mice. Data are presented as dot plot with median; $n = 7$. Student's t test: *, $P < 0.05$.

of these pathways. However, whether myeloid cell infiltration occurs in the CNS of PD patients remains elusive.

In this study we demonstrate that after MPTP intoxication, DNs are not killed through direct CD95-mediated cell death. In contrast, specific deletion of CD95L in myeloid cells and pharmacological neutralization of CD95L in the periphery prevented MPTP-induced degeneration of DNs, by interfering with the innate immune response. Indeed, this study highlights the importance of the peripheral innate immune response in the progression of neurodegeneration and identifies the CD95/CD95L system as a crucial trigger of this inflammatory response in neurodegeneration. Thus, we propose systemic neutralization of CD95L as a potential therapy in neurodegeneration.

MATERIALS AND METHODS

Animals. C57BL/6J mice were purchased from Charles River or Harlan Laboratories, Inc. *FasL-floxed* mice (Karray et al., 2004) were bred with *LysM^{cre}* mice (The Jackson Laboratory). *Fas-floxed* mice (gift from K. Rajewsky, Max-Delbrück-Centrum für Molekulare Medizin, Berlin-Buch, Germany) were bred with *DAT^{cre}* mice (The Jackson Laboratory). tdTomato-*Rosa26-flox* mice (The Jackson Laboratory) were bred with *Cx3cr1^{creER}* (Yona et al., 2013) mice. All floxed and Cre mouse lines were backcrossed with C57BL/6J for >10 generations. The induction of Cre recombinase in tdTomato$^{R26f/f;Cx3cr1creER}$ mice was performed as previously described (Goldmann et al., 2013). tdTomato$^{R26f/f;Cx3cr1creER}$ mice were used for MPTP intoxication 6 wk after tamoxifen induction. Experimental animals were age matched and used at 8–10 or 10–12 wk of age. All animal experiments were performed in accordance with institutional guidelines of the German Cancer Research Center and were approved by the Regierungspräsidium Karlsruhe.

Administration of MPTP. For MPTP intoxication, mice received five i.p. injections of 30 mg/kg bodyweight MPTP (free base) dissolved in 0.9% saline on five consecutive days. The control mice were injected with saline only.

Pharmacological blockade of CD95. Directly after the first and fifth MPTP injection, mice were intravenously injected with 50 µg APG112 (dissolved in 200 µl sterile PBS; Apogenix). APG112 is a human CD95-Fc fusion protein with a point mutation in the CH2 domain deleting the endogenous glycosylation site. Therefore, APG112 can neutralize CD95 activity by binding to CD95L with the lack of FcγR binding capability.

Generation of BM chimeric mice. BM chimeric mice were generated according to previously reported studies with modifications (Cui et al., 2002; Mildner et al., 2007). Irradiation was carried with a Gammacell 40 Exactor Low Dose-Rate Research Irradiator. Under anesthesia, the mouse head was covered by two lead stripes to protect the brain from irradiation, and the rest of the mouse body was exposed to parallel opposed fields of irradiation with a total dose of 13 Gy, which was split into two exposure of 6.5 Gy with a 4-h interval. 4×10^6 *CD95L$^{f/f;LysMcre\pm}$* BM cells were injected into the tail vein of recipient mice (C57BL/6, CD45.1, 4–5 wk old) within 24 h after irradiation. BM reconstitution levels were evaluated by FACS analysis of peripheral blood 7 wk after transplantation, and mice were used for MPTP intoxication 8 wk after transplantation.

Tissue preparation. At the described time points, mice were deeply anesthetized by i.p. injection of a ketamine/rompun mixture (85 mg/kg and 13 mg/kg) for tissue preparation. Blood samples were collected by heart puncture for FACS staining. After blood sampling, mice were transcardially perfused with 25 ml HBSS (Invitrogen) and then 25 ml of 4% paraformaldehyde (PFA) for fixation. Brains were fixed overnight with 4% PFA and then sectioned at 50-µm coronal slices using a VT1200 vibratome (Leica). 30 coronal serial sections covering the whole SNpc were obtained from each animal. Every fourth section was chosen among the 30 serial sections of each animal, and in total, 6 sections were used for staining of each animal.

Flow cytometry and cell sorting. Erythrocytes were lysed using lysing buffer (BD), and cells were preblocked with anti-CD16/CD32 (Fc Block; eBioscience). Cells were stained on ice for 20 min with combinations of anti-CD45 (APC-Cy7; eBioscience), anti-Ly6C (PerCP-Cy5.5; eBioscience), anti-CD11b (APC; BD), biotinylated anti-CD115 (followed by secondary staining with streptavidin-PE-Cy7; eBioscience), and anti-CD43 (PE; BD) as positive markers and FITC-conjugated lineage markers (CD4, CD19, Ly6G, and Nk1.1; BD) as dump markers for monocytes. For evaluating the reconstitution of chimeric mice, blood cells were stained with anti-CD45.1 (FITC; BD) and anti-CD45.2 (PE-Cy7; BD). Flow cytometry was performed on a FACSCanto II flow cytometer (BD), and FACS data were analyzed with FlowJo Software (Tree Star).

Immunohistochemistry staining. Midbrain sections (50 µm) were immunostained for anti-TH (EMD Millipore), which was followed by incubation with HRP-conjugated secondary antibody, and visualized by diaminobenzidine (DAB) staining. Sections were counterstained with thionin solution (Nissl stain).

Midbrain sections (50 µm) were blocked and permeabilized in PBS buffer containing 0.3% horse serum and 0.25% Triton X-100 for 1 h and then immunostained for 48 h with a combination of TH (EMD Millipore), CD11b (Abcam or eBioscience)/Iba1 (Wako Pure Chemical Industries), and $P2Y_{12}$ (gift from D. Julius, University of California, San Francisco, San Francisco, CA)/CD169 (AbD Serotec) or combination of TH and CD11b (eBioscience). Adequate Alexa Fluor–conjugated secondary antibodies were used for detection by immunofluorescence microscopy. DNs were assessed as TH^+. Resident microglia were identified as $CD11b^+P2Y_{12}^+$ or $Iba1^+CD169^-$ and infiltrating monocytes as $CD11b^+P2Y_{12}^-$ or $Iba1^+CD169^+$. In MPTP-injected $tdTomato^{R26f/f;Cx3cr1creER}$ mice, infiltrating monocytes were assessed as $CD11b^+tdTomato^-$ cells.

Analysis of striatal monoamine levels and MPTP metabolism. Measurement of striatal monoamine levels and MPTP metabolism was performed as previously described (Frank et al., 2012). In brief, on the day of the assay, striata were quickly dissected on ice and homogenized. DA, DOPAC, and HVA were quantified by HPLC with electrochemical detection. For measuring the MPTP metabolism, mice were given i.p. injections with 30 mg/kg MPTP (free base) and killed 90 min later. Striata were quickly dissected and homogenized. Levels of MPP^+ were determined by HPLC.

Image and data analysis. DAB-immunostained sections were recorded with a DM LB2 wide-field microscope (Leica). Immunofluorescent sections were recorded with a TCS SP5 confocal microscope (Leica).

For stereological analysis, investigators were blind for the genetic background and treatment of the animals. TH^+ cells on sections were counted manually with the ImageJ Cell Counter Plugin (National Institutes of Health). Positive cells were marked and the markers were saved for rechecking. Stained DNs within the VTA were not included.

For analysis of CD11b staining, CD11b-positive and CD11b single-positive area within the SNpc were measured with the ImageJ Threshold Color Plugin. For analysis of $CD11b^+P2Y_{12}^-$ area, image channels were merged (cyan for TH, green for $P2Y_{12}$, and red for CD11b), and only the area of SNpc with TH^+ cells was chosen for analysis. $CD11b^+P2Y_{12}^-$ area was analyzed with the ImageJ Threshold Color Plugin according to the instructions. All images were analyzed with the same setting of color threshold.

Statistics. Statistical significance of all endpoints was evaluated by one-way ANOVA with Newman–Keuls multi-comparison post-hoc test for analysis of multiple groups or Student's *t* test for analysis of two groups, unless indicated otherwise. Data are presented as mean ± SEM or dot plot with median. Statistical significance was reported by the p-value of the statistical test procedures and was, unless otherwise indicated, assessed as significant (*, $P < 0.05$), strongly significant (**, $P < 0.01$), or highly significant (***, $P < 0.001$). All statistical analyses were performed with Prism software (version 5; GraphPad Software).

We thank Sabine Ceremella (Department of Neurology, Göttingen University, Göttingen, Germany) for assistance with MPTP intoxication in mice and Stefanie Limpert (Division of Molecular Neurobiology, German Cancer Research Center [DKFZ], Heidelberg, Germany), Jens Lang, Dr. Kerstin Dell, and Dr. Michaela Socher (Animal Facility, DKFZ) for their aid with generating BM chimeric mice. And we also appreciate Prof. David Julius for sharing with us the anti-$P2Y_{12}$ antibody.

This work was funded by the DKFZ and the Federal Ministry of Education and Research (BioRN-INB-07).

The authors declare no competing financial interests.

Submitted: 21 November 2013
Accepted: 26 February 2015

REFERENCES

Adachi, M., S. Suematsu, T. Suda, D. Watanabe, H. Fukuyama, J. Ogasawara, T. Tanaka, N. Yoshida, and S. Nagata. 1996. Enhanced and accelerated lymphoproliferation in Fas-null mice. *Proc. Natl. Acad. Sci. USA*. 93: 2131–2136. http://dx.doi.org/10.1073/pnas.93.5.2131

Ahmed, I., R. Tamouza, M. Delord, R. Krishnamoorthy, C. Tzourio, C. Mulot, M. Nacfer, J.-C. Lambert, P. Beaune, P. Laurent-Puig, et al. 2012. Association between Parkinson's disease and the HLA-DRB1 locus. *Mov. Disord.* 27:1104–1110. http://dx.doi.org/10.1002/mds.25035

Ajami, B., J.L. Bennett, C. Krieger, K.M. McNagny, and F.M.V. Rossi. 2011. Infiltrating monocytes trigger EAE progression, but do not contribute to the resident microglia pool. *Nat. Neurosci.* 14:1142–1149. http://dx.doi.org/10.1038/nn.2887

Brochard, V., B. Combadière, A. Prigent, Y. Laouar, A. Perrin, V. Beray-Berthat, O. Bonduelle, D. Alvarez-Fischer, J. Callebert, J.M. Launay, et al. 2009. Infiltration of CD4+ lymphocytes into the brain contributes to neurodegeneration in a mouse model of Parkinson disease. *J. Clin. Invest.* 119:182–192. http://dx.doi.org/10.1172/JCI36470

Butovsky, O., S. Siddiqui, G. Gabriely, A.J. Lanser, B. Dake, G. Murugaiyan, C.E. Doykan, P.M. Wu, R.R. Gali, L.K. Iyer, et al. 2012. Modulating inflammatory monocytes with a unique microRNA gene signature ameliorates murine ALS. *J. Clin. Invest.* 122:3063–3087. http://dx.doi.org/10.1172/JCI62636

Butovsky, O., M.P. Jedrychowski, C.S. Moore, R. Cialic, A.J. Lanser, G. Gabriely, T. Koeglsperger, B. Dake, P.M. Wu, C.E. Doykan, et al. 2014. Identification of a unique TGF-β–dependent molecular and functional signature in microglia. *Nat. Neurosci.* 17:131–143. http://dx.doi.org/10.1038/nn.3599

Cho, I.-H., J. Hong, E.C. Suh, J.H. Kim, H. Lee, J.E. Lee, S. Lee, C.-H. Kim, D.W. Kim, E.-K. Jo, et al. 2008. Role of microglial IKKβ in kainic acid-induced hippocampal neuronal cell death. *Brain.* 131:3019–3033. http://dx.doi.org/10.1093/brain/awn230

Corsini, N.S., I. Sancho-Martinez, S. Laudenklos, D. Glagow, S. Kumar, E. Letellier, P. Koch, M. Teodorczyk, S. Kleber, S. Klussmann, et al. 2009. The death receptor CD95 activates adult neural stem cells for working memory formation and brain repair. *Cell Stem Cell.* 5:178–190. http://dx.doi.org/10.1016/j.stem.2009.05.004

Cros, J., N. Cagnard, K. Woollard, N. Patey, S.-Y. Zhang, B. Senechal, A. Puel, S.K. Biswas, D. Moshous, C. Picard, et al. 2010. Human $CD14^{dim}$ monocytes patrol and sense nucleic acids and viruses via TLR7 and TLR8 receptors. *Immunity.* 33:375–386. http://dx.doi.org/10.1016/j.immuni.2010.08.012

Cui, Y.-Z., H. Hisha, G.-X. Yang, T.-X. Fan, T. Jin, Q. Li, Z. Lian, and S. Ikehara. 2002. Optimal protocol for total body irradiation for allogeneic bone marrow transplantation in mice. *Bone Marrow Transplant.* 30:843–849. http://dx.doi.org/10.1038/sj.bmt.1703766

Członkowska, A., M. Kohutnicka, I. Kurkowska-Jastrzębska, and A. Członkowski. 1996. Microglial reaction in MPTP (1-methyl-4-phenyl-1,2,3,6-tetrahydropyridine) induced Parkinson's disease mice model. *Neurodegeneration.* 5:137–143. http://dx.doi.org/10.1006/neur.1996.0020

Dauer, W., and S. Przedborski. 2003. Parkinson's disease: mechanisms and models. *Neuron.* 39:889–909. http://dx.doi.org/10.1016/S0896-6273(03)00568-3

Demjen, D., S. Klussmann, S. Kleber, C. Zuliani, B. Stieltjes, C. Metzger, U.A. Hirt, H. Walczak, W. Falk, M. Essig, et al. 2004. Neutralization of CD95 ligand promotes regeneration and functional recovery after spinal cord injury. *Nat. Med.* 10:389–395. http://dx.doi.org/10.1038/nm1007

Desbarats, J., R.B. Birge, M. Mimouni-Rongy, D.E. Weinstein, J.-S. Palerme, and M.K. Newell. 2003. Fas engagement induces neurite growth through ERK activation and p35 upregulation. *Nat. Cell Biol.* 5:118–125. http://dx.doi.org/10.1038/ncb916

Diserbo, M., A. Agin, I. Lamproglou, J. Mauris, F. Staali, E. Multon, and C. Amourette. 2002. Blood-brain barrier permeability after gamma whole-body irradiation: an in vivo microdialysis study. *Can. J. Physiol. Pharmacol.* 80:670–678. http://dx.doi.org/10.1139/y02-070

Ferrer, I., R. Blanco, B. Cutillas, and S. Ambrosio. 2000. Fas and Fas-L expression in Huntington's disease and Parkinson's disease. *Neuropathol. Appl. Neurobiol.* 26:424–433. http://dx.doi.org/10.1046/j.1365-2990.2000.00267.x

Frank, T., F. Klinker, B.H. Falkenburger, R. Laage, F. Lühder, B. Göricke, A. Schneider, H. Neurath, H. Desel, D. Liebetanz, et al. 2012. Pegylated granulocyte colony-stimulating factor conveys long-term neuroprotection and improves functional outcome in a model of Parkinson's disease. *Brain*. 135:1914–1925. http://dx.doi.org/10.1093/brain/aws054

Funk, N., P. Wieghofer, S. Grimm, R. Schaefer, H.-J. Bühring, T. Gasser, and S. Biskup. 2013. Characterization of peripheral hematopoietic stem cells and monocytes in Parkinson's disease. *Mov. Disord*. 28:392–395. http://dx.doi.org/10.1002/mds.25300

Gao, X., H. Chen, M.A. Schwarzschild, and A. Ascherio. 2011. Use of ibuprofen and risk of Parkinson disease. *Neurology*. 76:863–869. http://dx.doi.org/10.1212/WNL.0b013e31820f2d79

Ginhoux, F., M. Greter, M. Leboeuf, S. Nandi, P. See, S. Gokhan, M.F. Mehler, S.J. Conway, L.G. Ng, E.R. Stanley, et al. 2010. Fate mapping analysis reveals that adult microglia derive from primitive macrophages. *Science*. 330:841–845. http://dx.doi.org/10.1126/science.1194637

Goldmann, T., P. Wieghofer, P.F. Müller, Y. Wolf, D. Varol, S. Yona, S.M. Brendecke, K. Kierdorf, O. Staszewski, M. Datta, et al. 2013. A new type of microglia gene targeting shows TAK1 to be pivotal in CNS autoimmune inflammation. *Nat. Neurosci*. 16:1618–1626. http://dx.doi.org/10.1038/nn.3531

Grozdanov, V., C. Bliederhaeuser, W.P. Ruf, V. Roth, K. Fundel-Clemens, L. Zondler, D. Brenner, A. Martin-Villalba, B. Hengerer, J. Kassubek, et al. 2014. Inflammatory dysregulation of blood monocytes in Parkinson's disease patients. *Acta Neuropathol*. 128:651–663. http://dx.doi.org/10.1007/s00401-014-1345-4

Hayley, S., S.J. Crocker, P.D. Smith, T. Shree, V. Jackson-Lewis, S. Przedborski, M. Mount, R. Slack, H. Anisman, and D.S. Park. 2004. Regulation of dopaminergic loss by Fas in a 1-methyl-4-phenyl-1,2,3,6-tetrahydropyridine model of Parkinson's disease. *J. Neurosci*. 24:2045–2053. http://dx.doi.org/10.1523/JNEUROSCI.4564-03.2004

Haynes, S.E., G. Hollopeter, G. Yang, D. Kurpius, M.E. Dailey, W.-B. Gan, and D. Julius. 2006. The P2Y12 receptor regulates microglial activation by extracellular nucleotides. *Nat. Neurosci*. 9:1512–1519. http://dx.doi.org/10.1038/nn1805

Karray, S., C. Kress, S. Cuvellier, C. Hue-Beauvais, D. Damotte, C. Babinet, and M. Lévi-Strauss. 2004. Complete loss of *Fas ligand* gene causes massive lymphoproliferation and early death, indicating a residual activity of *gld* allele. *J. Immunol*. 172:2118–2125. http://dx.doi.org/10.4049/jimmunol.172.4.2118

Kierdorf, K., D. Erny, T. Goldmann, V. Sander, C. Schulz, E.G. Perdiguero, P. Wieghofer, A. Heinrich, P. Riemke, C. Hölscher, et al. 2013a. Microglia emerge from erythromyeloid precursors via Pu.1- and Irf8-dependent pathways. *Nat. Neurosci*. 16:273–280. http://dx.doi.org/10.1038/nn.3318

Kierdorf, K., N. Katzmarski, C.A. Haas, and M. Prinz. 2013b. Bone marrow cell recruitment to the brain in the absence of irradiation or parabiosis bias. *PLoS ONE*. 8:e58544. http://dx.doi.org/10.1371/journal.pone.0058544

Kleber, S., I. Sancho-Martinez, B. Wiestler, A. Beisel, C. Gieffers, O. Hill, M. Thiemann, W. Mueller, J. Sykora, A. Kuhn, et al. 2008. Yes and PI3K bind CD95 to signal invasion of glioblastoma. *Cancer Cell*. 13:235–248. http://dx.doi.org/10.1016/j.ccr.2008.02.003

Kokovay, E., and L.A. Cunningham. 2005. Bone marrow-derived microglia contribute to the neuroinflammatory response and express iNOS in the MPTP mouse model of Parkinson's disease. *Neurobiol. Dis*. 19:471–478. http://dx.doi.org/10.1016/j.nbd.2005.01.023

Landau, A.M., K.C. Luk, M.-L. Jones, R. Siegrist-Johnstone, Y.K. Young, E. Kouassi, V.V. Rymar, A. Dagher, A.F. Sadikot, and J. Desbarats. 2005. Defective Fas expression exacerbates neurotoxicity in a model of Parkinson's disease. *J. Exp. Med*. 202:575–581. http://dx.doi.org/10.1084/jem.20050163

Letellier, E., S. Kumar, I. Sancho-Martinez, S. Krauth, A. Funke-Kaiser, S. Laudenklos, K. Konecki, S. Klussmann, N.S. Corsini, S. Kleber, et al. 2010. CD95-ligand on peripheral myeloid cells activates Syk kinase to trigger their recruitment to the inflammatory site. *Immunity*. 32:240–252. http://dx.doi.org/10.1016/j.immuni.2010.01.011

Leuschner, F., P. Dutta, R. Gorbatov, T.I. Novobrantseva, J.S. Donahoe, G. Courties, K.M. Lee, J.I. Kim, J.F. Markmann, B. Marinelli, et al. 2011. Therapeutic siRNA silencing in inflammatory monocytes in mice. *Nat. Biotechnol*. 29:1005–1010. http://dx.doi.org/10.1038/nbt.1989

Liberatore, G.T., V. Jackson-Lewis, S. Vukosavic, A.S. Mandir, M. Vila, W.G. McAuliffe, V.L. Dawson, T.M. Dawson, and S. Przedborski. 1999. Inducible nitric oxide synthase stimulates dopaminergic neurodegeneration in the MPTP model of Parkinson disease. *Nat. Med*. 5:1403–1409. http://dx.doi.org/10.1038/70978

Martin-Villalba, A., E. Llorens-Bobadilla, and D. Wollny. 2013. CD95 in cancer: tool or target? *Trends Mol. Med*. 19:329–335. http://dx.doi.org/10.1016/j.molmed.2013.03.002

McGeer, P.L., and E.G. McGeer. 2008. Glial reactions in Parkinson's disease. *Mov. Disord*. 23:474–483. http://dx.doi.org/10.1002/mds.21751

Mildner, A., H. Schmidt, M. Nitsche, D. Merkler, U.-K. Hanisch, M. Mack, M. Heikenwalder, W. Brück, J. Priller, and M. Prinz. 2007. Microglia in the adult brain arise from Ly-6C^{hi}CCR2^{+} monocytes only under defined host conditions. *Nat. Neurosci*. 10:1544–1553. http://dx.doi.org/10.1038/nn2015

Mildner, A., M. Mack, H. Schmidt, W. Brück, M. Djukic, M.D. Zabel, A. Hille, J. Priller, and M. Prinz. 2009. CCR2^{+}Ly-6C^{hi} monocytes are crucial for the effector phase of autoimmunity in the central nervous system. *Brain*. 132:2487–2500. http://dx.doi.org/10.1093/brain/awp144

Mildner, A., B. Schlevogt, K. Kierdorf, C. Böttcher, D. Erny, M.P. Kummer, M. Quinn, W. Brück, I. Bechmann, M.T. Heneka, et al. 2011. Distinct and non-redundant roles of microglia and myeloid subsets in mouse models of Alzheimer's disease. *J. Neurosci*. 31:11159–11171. http://dx.doi.org/10.1523/JNEUROSCI.6209-10.2011

Mogi, M., M. Harada, T. Kondo, Y. Mizuno, H. Narabayashi, P. Riederer, and T. Nagatsu. 1996. The soluble form of Fas molecule is elevated in parkinsonian brain tissues. *Neurosci. Lett*. 220:195–198. http://dx.doi.org/10.1016/S0304-3940(96)13257-2

Peter, M.E., R.C. Budd, J. Desbarats, S.M. Hedrick, A.-O. Hueber, M.K. Newell, L.B. Owen, R.M. Pope, J. Tschopp, H. Wajant, et al. 2007. The CD95 receptor: apoptosis revisited. *Cell*. 129:447–450. http://dx.doi.org/10.1016/j.cell.2007.04.031

Priller, J., A. Flügel, T. Wehner, M. Boentert, C.A. Haas, M. Prinz, F. Fernández-Klett, K. Prass, I. Bechmann, B.A. de Boer, et al. 2001. Targeting gene-modified hematopoietic cells to the central nervous system: use of green fluorescent protein uncovers microglial engraftment. *Nat. Med*. 7:1356–1361. http://dx.doi.org/10.1038/nm1201-1356

Prinz, M., and A. Mildner. 2011. Microglia in the CNS: immigrants from another world. *Glia*. 59:177–187. http://dx.doi.org/10.1002/glia.21104

Ransohoff, R.M., and A.E. Cardona. 2010. The myeloid cells of the central nervous system parenchyma. *Nature*. 468:253–262. http://dx.doi.org/10.1038/nature09615

Rodriguez, M., L. Alvarez-Erviti, F.J. Blesa, M.C. Rodríguez-Oroz, A. Arina, I. Melero, L.I. Ramos, and J.A. Obeso. 2007. Bone-marrow-derived cell differentiation into microglia: a study in a progressive mouse model of Parkinson's disease. *Neurobiol. Dis*. 28:316–325. http://dx.doi.org/10.1016/j.nbd.2007.07.024

Ros-Bernal, F., S. Hunot, M.T. Herrero, S. Parnadeau, J.-C. Corvol, L. Lu, D. Alvarez-Fischer, M.A. Carrillo-de Sauvage, F. Saurini, C. Coussieu, et al. 2011. Microglial glucocorticoid receptors play a pivotal role in regulating dopaminergic neurodegeneration in parkinsonism. *Proc. Natl. Acad. Sci. USA*. 108:6632–6637. http://dx.doi.org/10.1073/pnas.1017820108

Roths, J.B., E.D. Murphy, and E.M. Eicher. 1984. A new mutation, gld, that produces lymphoproliferation and autoimmunity in C3H/HeJ mice. *J. Exp. Med*. 159:1–20. http://dx.doi.org/10.1084/jem.159.1.1

Schulz, C., E. Gomez Perdiguero, L. Chorro, H. Szabo-Rogers, N. Cagnard, K. Kierdorf, M. Prinz, B. Wu, S.E.W. Jacobsen, J.W. Pollard, et al. 2012. A lineage of myeloid cells independent of Myb and hematopoietic stem cells. *Science*. 336:86–90. http://dx.doi.org/10.1126/science.1219179

Simunovic, F., M. Yi, Y. Wang, L. Macey, L.T. Brown, A.M. Krichevsky, S.L. Andersen, R.M. Stephens, F.M. Benes, and K.C. Sonntag. 2009. Gene expression profiling of substantia nigra dopamine neurons: further insights into Parkinson's disease pathology. *Brain*. 132:1795–1809. http://dx.doi.org/10.1093/brain/awn323

Taylor, D.L., F. Jones, E.S.F.C.S. Kubota, and J.M. Pocock. 2005. Stimulation of microglial metabotropic glutamate receptor mGlu2 triggers tumor necrosis factor α-induced neurotoxicity in concert with microglial-derived

Fas ligand. *J. Neurosci.* 25:2952–2964. http://dx.doi.org/10.1523/JNEUROSCI.4456-04.2005

Terrazzino, S., A. Bauleo, A. Baldan, and A. Leon. 2002. Peripheral LPS administrations up-regulate Fas and FasL on brain microglial cells: a brain protective or pathogenic event? *J. Neuroimmunol.* 124:45–53. http://dx.doi.org/10.1016/S0165-5728(02)00013-9

Venderova, K., and D.S. Park. 2012. Programmed cell death in Parkinson's disease. *Cold Spring Harb. Perspect. Med.* 2:a009365. http://dx.doi.org/10.1101/cshperspect.a009365

Wu, D.C., V. Jackson-Lewis, M. Vila, K. Tieu, P. Teismann, C. Vadseth, D.K. Choi, H. Ischiropoulos, and S. Przedborski. 2002. Blockade of microglial activation is neuroprotective in the 1-methyl-4-phenyl-1,2,3,6-tetrahydropyridine mouse model of Parkinson disease. *J. Neurosci.* 22:1763–1771.

Yona, S., and S. Jung. 2010. Monocytes: subsets, origins, fates and functions. *Curr. Opin. Hematol.* 17:53–59. http://dx.doi.org/10.1097/MOH.0b013e3283324f80

Yona, S., K.-W. Kim, Y. Wolf, A. Mildner, D. Varol, M. Breker, D. Strauss-Ayali, S. Viukov, M. Guilliams, A. Misharin, et al. 2013. Fate mapping reveals origins and dynamics of monocytes and tissue macrophages under homeostasis. *Immunity.* 38:79–91. http://dx.doi.org/10.1016/j.immuni.2012.12.001

Zuliani, C., S. Kleber, S. Klussmann, T. Wenger, M. Kenzelmann, N. Schreglmann, A. Martinez, J.A. del Rio, E. Soriano, P. Vodrazka, et al. 2006. Control of neuronal branching by the death receptor CD95 (Fas/Apo-1). *Cell Death Differ.* 13:31–40. http://dx.doi.org/10.1038/sj.cdd.4401720